



Room 14-0551  
77 Massachusetts Avenue  
Cambridge, MA 02139  
Ph: 617.253.5668 Fax: 617.253.1690  
Email: docs@mit.edu  
<http://libraries.mit.edu/docs>

## **DISCLAIMER OF QUALITY**

Due to the condition of the original material, there are unavoidable flaws in this reproduction. We have made every effort possible to provide you with the best copy available. If you are dissatisfied with this product and find it unusable, please contact Document Services as soon as possible.

Thank you.

**Some pages in the original document contain color pictures or graphics that will not scan or reproduce well.**

Design and Testing of the Thermal Properties of the Structure of an Ultra High-Throughput Mutational Spectrometer

by

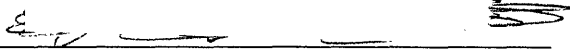
Michael R. Del Zio

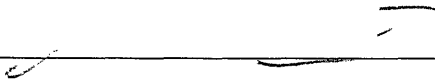
SUBMITTED TO THE DEPARTMENT OF MECHANICAL ENGINEERING IN PARTIAL FULFILLMENT OF THE REQUIREMENTS FOR THE DEGREE OF


BACHELOR OF SCIENCE IN MECHANICAL ENGINEERING AT THE MASSACHUSETTS INSTITUTE OF TECHNOLOGY

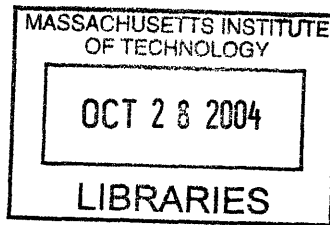
JUNE 2004

© 2004 Massachusetts Institute of Technology  
All rights reserved

Signature of Author   
Department of Mechanical Engineering  
May 7, 2004

Certified by   
Ian W. Hunter  
Hatsopoulos Professor of Mechanical Engineering  
Thesis Supervisor

Accepted by   
Ernest G. Cravalho  
Chairman of the Undergraduate Thesis Committee, Mechanical Engineering



ARCHIVES

# Design and Testing of the Thermal Properties of the Structure of an Ultra High-Throughput Mutational Spectrometer

by

Michael R. Del Zio

Submitted to the Department of Mechanical Engineering  
on May 7, 2004 in partial fulfillment of the requirements  
for the Degree of Bachelor of Science in Mechanical Engineering

## ABSTRACT

A process known as mutational spectrometry allows the detection of both single and multiple mutations that appear to be spontaneous, using a technique known as constant denaturing capillary electrophoresis (CDCE). CDCE requires a region of constant temperature and concentration of denaturant. A massively parallel, fully automated instrument, capable of handling as many as 10,000 DNA samples simultaneously, is suited to this technique. A modular structure of such a mutational spectrometer was designed to remain water-tight, provide an array to hold the capillaries for electrophoretic excitation, and modulate the flow of a heat transfer fluid. Six such modules were manufactured and assembled. As the heat transfer fluid passed through the assembled structure, the natural thermal loss was determined.

Thesis Supervisor: Ian W. Hunter

Title: Hatsopoulos Professor of Mechanical Engineering

## **Acknowledgements**

I would like to thank Professor Ian Hunter, Dr. Andrew Taberner, Bryan Crane, Craig Forest, Tim Fofonoff, and Nathan Ball for all their help in this project.

## Table of Contents

<b>1.0 Introduction</b> .....	<b>6</b>
<b>2.0 Mutation Detection</b> .....	<b>6</b>
<b>2.1 Instrumentation Needs</b> .....	<b>7</b>
<b>2.2 Differences in Electrophoretic Mobility</b> .....	<b>7</b>
<b>and Capillary Electrophoresis</b>	
<b>2.2.1 Types of Capillary Electrophoresis</b> .....	<b>8</b>
<b>2.3 Mutational Spectrometry</b> .....	<b>9</b>
<b>3.0 Instrument Concept</b> .....	<b>10</b>
<b>3.1 Design Requirements of the Main Structure</b> .....	<b>11</b>
<b>4.0 Design of the Modular Structure</b> .....	<b>12</b>
<b>4.1 Capillary Arrays</b> .....	<b>13</b>
<b>4.2 Flow Restrictor Arrays</b> .....	<b>15</b>
<b>4.3 Main Module</b> .....	<b>20</b>
<b>4.3.1 Proof of Concept</b> .....	<b>20</b>
<b>4.3.2 Main Module Design</b> .....	<b>22</b>
<b>4.4 Assembled Subunit</b> .....	<b>26</b>
<b>5.0 Manufacturing and Assembling the Subunit</b> .....	<b>28</b>
<b>5.1 Manufacturing the Capillary and Flow Restrictor Arrays</b> .....	<b>30</b>
<b>5.2 Manufacturing the Main Module</b> .....	<b>32</b>
<b>5.3 Assembling the Subunit</b> .....	<b>33</b>
<b>6.0 Testing of the Thermal Properties</b> .....	<b>34</b>
<b>6.1 Procedure</b> .....	<b>34</b>
<b>6.2 Results</b> .....	<b>37</b>
<b>6.3 Discussion</b> .....	<b>39</b>
<b>7.0 Conclusion</b> .....	<b>41</b>
<b>7.1 Future Work</b> .....	<b>41</b>
<b>Bibliography</b> .....	<b>42</b>

## Table of Figures

<b>1: Design schematic of an ultra high throughput mutational spectrometer</b> .....	<b>11</b>
<b>2: Pair of capillaries</b> .....	<b>12</b>
<b>3: Capillary array design</b> .....	<b>14</b>
<b>4: Capillary array under microscope</b> .....	<b>15</b>
<b>5: Flow restrictor arrays, wall thickness</b> .....	<b>17</b>
<b>6: Flow restrictor arrays, stock thickness</b> .....	<b>18</b>
<b>7: Flow restrictor array design</b> .....	<b>19</b>
<b>8: Preliminary design / proof of concept</b> .....	<b>21</b>
<b>9: Main module design</b> .....	<b>24</b>
<b>10: Bolt hole pattern on main module</b> .....	<b>25</b>
<b>11: Design of assembled subunit</b> .....	<b>27</b>
<b>12: Trotec laser machining system</b> .....	<b>28</b>
<b>13: Hass milling center</b> .....	<b>29</b>
<b>14: Wire electrical discharge machining (EDM) center</b> .....	<b>29</b>
<b>15: Microtap II tapping press</b> .....	<b>30</b>
<b>16: Machined capillary array</b> .....	<b>31</b>
<b>17: Machined flow restrictor array</b> .....	<b>31</b>
<b>18: Machined main module</b> .....	<b>33</b>
<b>19: Assembled subunit</b> .....	<b>34</b>
<b>20: Resistive thermal device (RTD)</b> .....	<b>35</b>
<b>21: Thermal experimental setup</b> .....	<b>36</b>
<b>22: RTD schematic</b> .....	<b>36</b>
<b>23: Temperature loss of structure in assumed operating range</b> .....	<b>40</b>
<b>24: Temperature loss as a function of the number of modules</b> .....	<b>40</b>

## **1.0 Introduction**

Existing DNA analyzers have been routinely used to detect mutations in DNA [20]. This has been a successful approach to gaining information about diseases, most of which are single DNA based mutations. In fact, of the four thousand known genetic diseases, three thousand are known to be caused by single base pair mutations. However, major diseases, such as cancer are not caused by single base pair mutations, but rather likely determined by multiple mutations. In order to discover these multiple mutations a new form of DNA analysis has been invented called mutational spectrometry. There are no commercially available mutational spectrometers and the few that have been developed only have a small number of channels and can only run a small number of DNA samples in parallel.

## **2.0 Mutation Detection**

Of the  $10^9$  base pairs that span the human genome, significantly less than 1% differs between individuals [20]. The differences include phenotypic qualities, such as physical looks, and also may account for differences in disease susceptibility. A disease that is caused by a single change in a unique base pair is called a point mutation. A single base pair mutation is a point mutation that can occur at very low frequencies in the population. These mutations account for a large portion of known diseases.

However, other diseases are caused by multiple mutations. During meiosis, chromosomes tend to link, resulting in genes in the same area being inherited together. This increases the probability of some combination of mutations to occur more frequently. Some of these combinations may account for diseases that are caused by multiple mutations.

## **2.1 Instrumentation Needs**

Gene sequencing is both a time consuming and expensive process [11]. In addition, detecting mutations by sequencing alone can be difficult due to the low frequency of occurrence. This instrument will use differences in electrophoretic mobility to detect mutated base pairs. Other methods of genetic analysis are not as well suited to mutations of low frequency of occurrence. Improved instrumentation could increase the speed of genetic analysis at significantly less cost. The technology should be able to handle a large-scale parallel configuration in conjunction with computer analysis. The instrument should be able to detect both single base pair and multiple mutations. Therefore, if extensive sequencing is necessary to study a particular mutation, the location of the mutation and number of base pairs involved may be known beforehand.

## **2.2 Differences in Electrophoretic Mobility and Capillary Electrophoresis**

Electrophoresis is the motion of a charged particle in an electric field. In studying DNA, electrophoresis is performed by placing a small sample of DNA in contact with a column of polyacrylamide gel, either in the form of a thick slab or the inner diameter of a capillary [25]. Since DNA has a net negative charge, if an electric potential is placed across the column the DNA will feel a net force toward the positive terminal. If the electric field is held constant, the velocity of the DNA through the column will be constant. There are two ways in which the DNA is separated as it moves through the column of gel. As the long strands of DNA move through the porous structure of the gel, the larger pieces are delayed due to the complexity of finding a path [12]. Alternatively, strands of DNA with different complexities have different melting



temperatures. If the samples are heated, the strands begin to melt and the structure folds over, inhibiting its motion through the column of gel.

Capillary electrophoresis has several advantages over slab gel electrophoresis. There is significantly better heat dissipation using capillaries, due to a greater surface area for a given electric potential. Therefore, smaller bore capillaries are more efficient in dissipating heat [14]. Since excessive heating can destroy DNA fragments, better cooling in the capillary format allows for higher electric potentials to be used safely. Thus, each run can take less time to complete. Also, capillary electrophoresis eliminates the need to pour slab gels, a time consuming and tedious process [7]. In addition, the capillary format is more suited to a massively parallel device using end-on detection of the capillaries.

### **2.2.1 Types of Capillary Electrophoresis**

There are two types of capillary electrophoresis that are suited to the instrument needs. Thermal gradient capillary electrophoresis (TGCE) utilizes the unique melting temperatures of different strands of DNA for separation. The spatial thermal gradient is established by controlling the end temperatures of a thermally conductive plate [4]. The presence of mutations is detected by the melting position of each particular strand. This method uses both a change in the mobility and a change in fluorescence of the strands to determine mutation. As the strands melt from a double helix into a random coil, a particular fluorescent dye changes intensity.

Constant denaturing capillary electrophoresis (CDCE) uses a zone of constant temperature and denaturant concentration to separate mutant from wild type alleles [11]. This technique also utilizes the principle that the electrophoretic mobility of a partially

melted molecule is reduced as compared to an unchanged molecule. Separation of DNA fragments containing a single base pair difference can be achieved by performing CDCE at a defined temperature [25]. The ability to vary the operating conditions provides a benefit over TGCE. The sensitivity of CDCE enables specific and precise detection of sequences over broad concentrations and low frequencies of occurrence [17]. The high-resolution separation of single base pair mutations makes CDCE extremely effective in detecting mutations that are spontaneous in nature [13]. The ability to detect random single base pair mutations successfully makes this technique useful in detecting multiple mutations.

### **2.3 Mutational Spectrometry**

The use of CDCE in mutation detection has determined the first mutational spectrum in human cells without phenotypic selection of mutants [17]. By detecting mutations without any prior knowledge, CDCE lends itself to spontaneous multiple mutations. Mutational spectrometry is the process by which mutant DNA sequences are separated from non-mutants on the basis of melting temperatures. The number of copies of mutant sequences is increased by DNA amplification, resulting in the observation of point mutations in biological samples at fractions at or above  $10^{-6}$  [10]. The advantage of mutational spectrometry is the ability to study sequences without any mutagen-specific information with a high level of sensitivity and specificity [21]. This technique has great potential for creating a large-scale parallel, fully automated instrument to determine mutation spectra.

### 3.0 Instrument Concept

The design for the ultra high throughput mutational spectrometer uses CDCE and end-on fluorescent detection with a high sensitivity camera. The device is massively parallel with the ability to handle as many as 10,000 samples simultaneously. The main structure of the instrument provides an array to hold the capillaries in the vertical orientation and uses a recirculating water bath as a temperature control system. Each capillary acts as an ohmic heating element due to resistive heating as the electric potential is applied. Coolant flows perpendicular to the length of the capillaries. The structure is divided up into 50.0 mm blocks, allowing the overall length of electrophoretic excitation to vary as necessary. The goal of this research was to design and build such a modular structure.

Near uniform intensity luminescence of the ends of the capillaries is achieved by a fluid-cooled overhead array of light emitting diodes (LED). The blue light from this array is collimated before reaching the capillaries. By collimating the light source, it is a good approximation that all the incoming intensity is unidirectional. The array of blue LEDs excites fluorescence from the ends of the capillaries and a half-silvered mirror, or beam splitter, directs the emitted light towards the high sensitivity, internally cooled camera, which is mounted horizontally. The camera is a charge coupled device (CCD) and uses light sensitive diodes to convert photons into electrons [2]. Thus, the greater the intensity of light, the more electric charge that is created by the diode. This camera is specifically sensitive to light in the blue range of the visible spectrum with a peak at 570 nm, which is known as its quantum efficiency. Given the high level of sensitivity of the

detection equipment, it is important that the instrument is light-sealed to the environment.

Figure 1 shows a schematic of the overall design of the instrument.

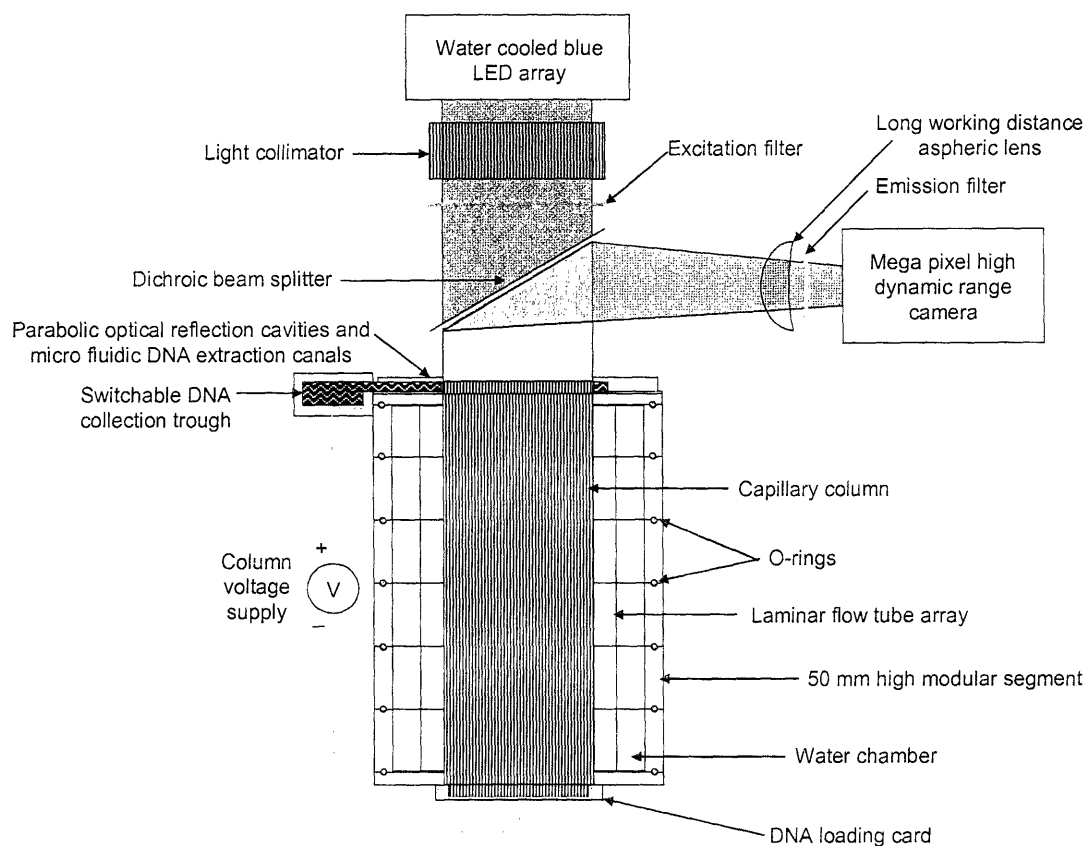


Figure 1: Design schematic of an ultra high throughput mutational spectrometer (taken from proposal from Bioinstrumentation Laboratory, MIT).

### 3.1 Design Requirements of the Main Structure

The design of the main structure must be in 50 mm high modular segments that connect in a water-tight fashion for temperature control using a heat transfer fluid. The design goal dictated a total length of 300 mm of electrophoretic excitation. The modules must be constructed from a material with a combination of high structural rigidity and high thermal conductivity, to aid in achieving a steady-state temperature. In order to maintain a constant and equal flow of coolant across each of the six segments of the

structure, some element inside the structure must resist a tendency for the water to flow unequally due to differences in pressure. Also, a modular design for a set of slides must be constructed to hold various arrays of capillaries for each segment. The capillaries are flexible with a 300  $\mu\text{m}$  outer diameter and a 75  $\mu\text{m}$  inner diameter. The capillaries need to be supported and held in alignment every 50 mm. Figure 2 shows a pair of capillaries.

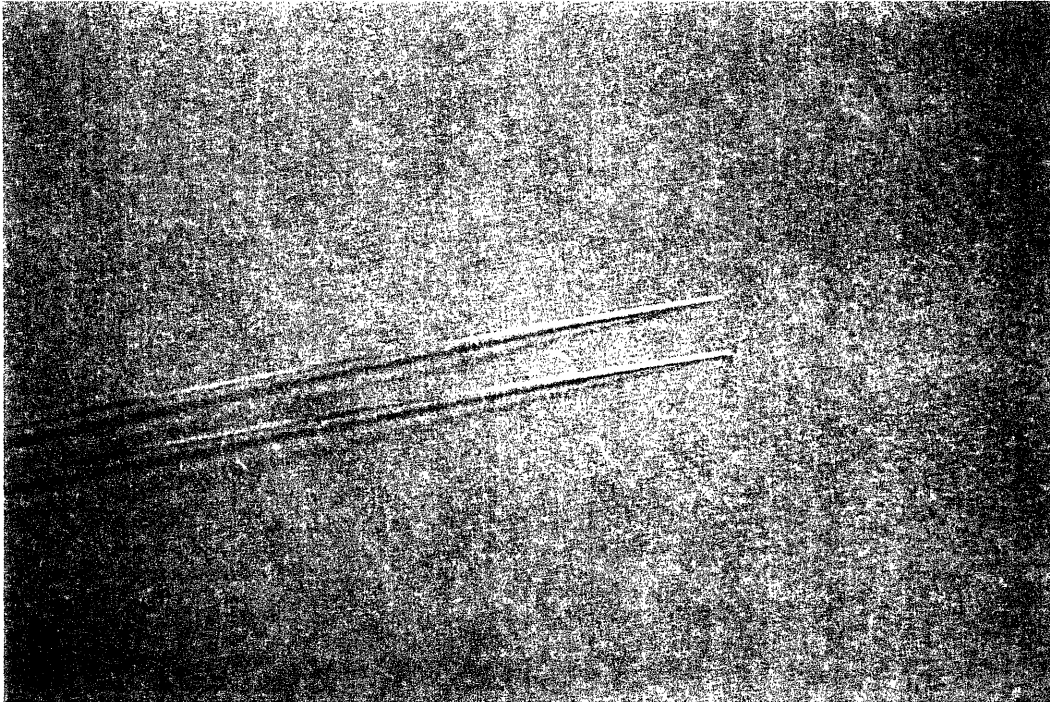


Figure 2: 300  $\mu\text{m}$  outer diameter, 75  $\mu\text{m}$  inner diameter polyamid coated, quartz capillaries.

#### **4.0 Design of the Modular Structure**

There were three main aspects to the design of the modular structure. First, the slide was designed to hold the array of 10,000 capillaries. Second, the arrays were designed that inhibit the flow of coolant within the structure. This was achieved by using a rectangular matrix of square holes to create effective impedance to the flow. The main structure was designed to house the arrays and allow for the temperature control system.

All the designs were created in the SolidEdge 3-D computer-aided drawing (CAD) environment [23].

#### **4.1 Capillary Arrays**

The maximum desired capillary density to be utilized in this instrument is a 100 by 100 array with 1 mm center-to-center spacing. This density is still within the limits of the detection equipment and keeps the size of the instrument reasonable. The holes were designed slightly oversized, with a diameter of 400  $\mu\text{m}$ , for ease of threading successive arrays of capillaries. A small border was left around the outer edges of the array for mounting. The design is shown in Figure 3.

Using considerations of the low need for structural rigidity, low cost, and manufacturing options, these slides were designed for manufacture in 3 mm thick acrylic. The chosen manufacturing process was the Epilog laser machining system, capable of the high resolution machining in plastics [6]. Figure 4 shows the quality of machining of an array of 400  $\mu\text{m}$  holes in diameter under a microscope.

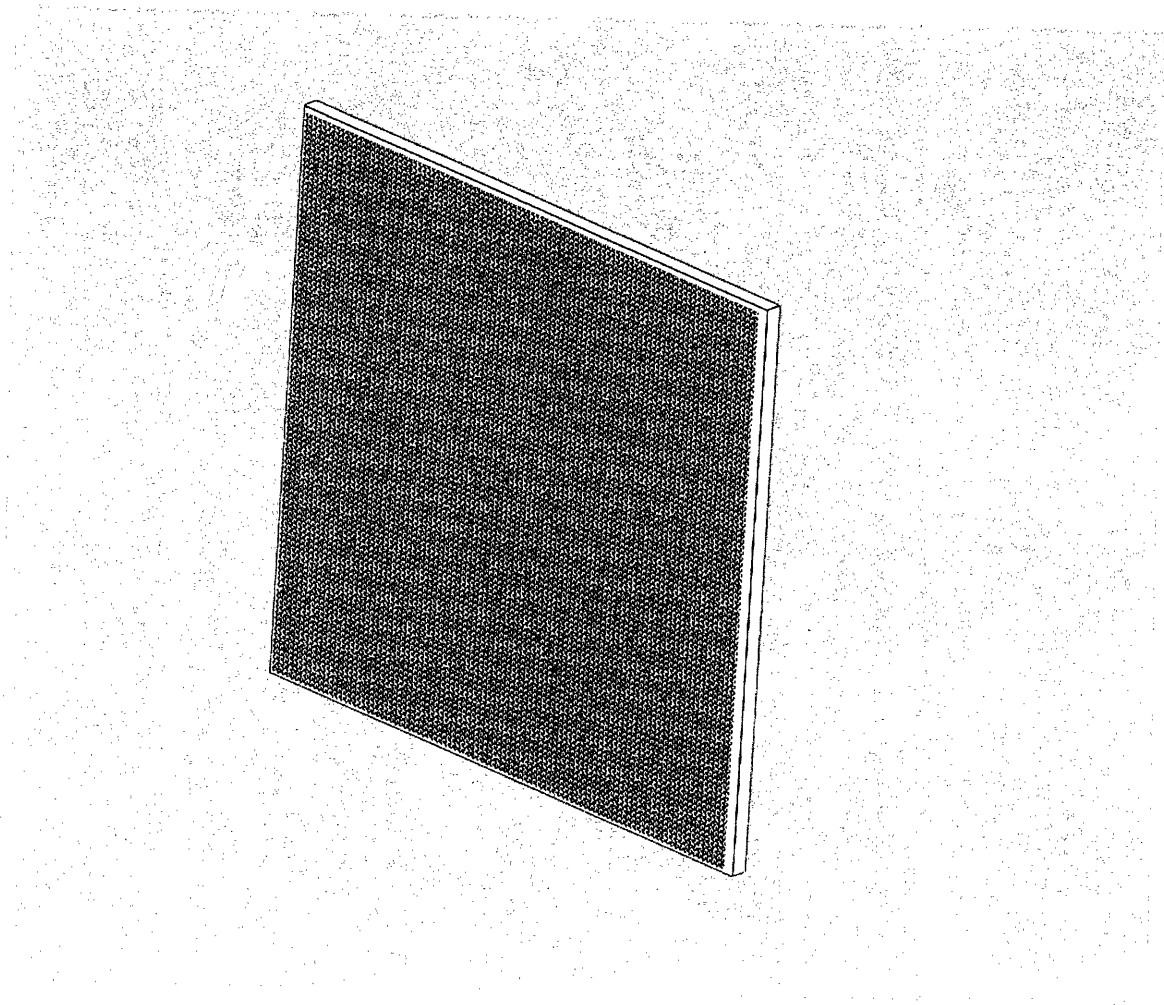


Figure 3: Capillary array design.



Figure 4: An array of holes 400  $\mu\text{m}$  in diameter.

#### **4.2 Flow Restrictor Arrays**

These plates are designed to sit vertically inside the main structure and restrict the flow of coolant perpendicular to the length of the capillaries. This ensures equal flow across each of the modules, regardless of their height in the structure. The coolant is forced to pass through an array of small square holes before flowing over the capillaries. The flow is restricted to due to viscous and turbulent loss [24]. The design uses one array of square holes to separate the region where the capillaries operate and the entrance side for the coolant and another for the exit side. This allows for a uniform flow across the length of the structure.

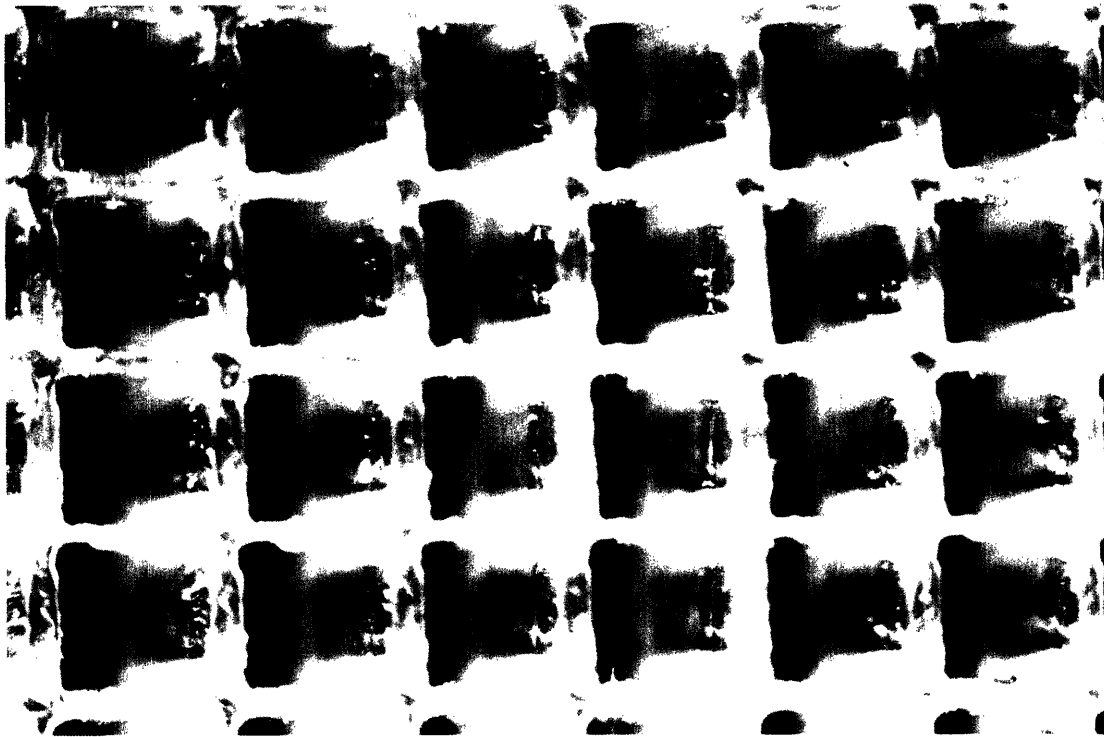
The design for these arrays was mostly dictated by machining limitations. These slides were also cut on the Epilog laser machining system in acrylic [6]. The design should balance several parameters to control the flow through the array. The flow can be



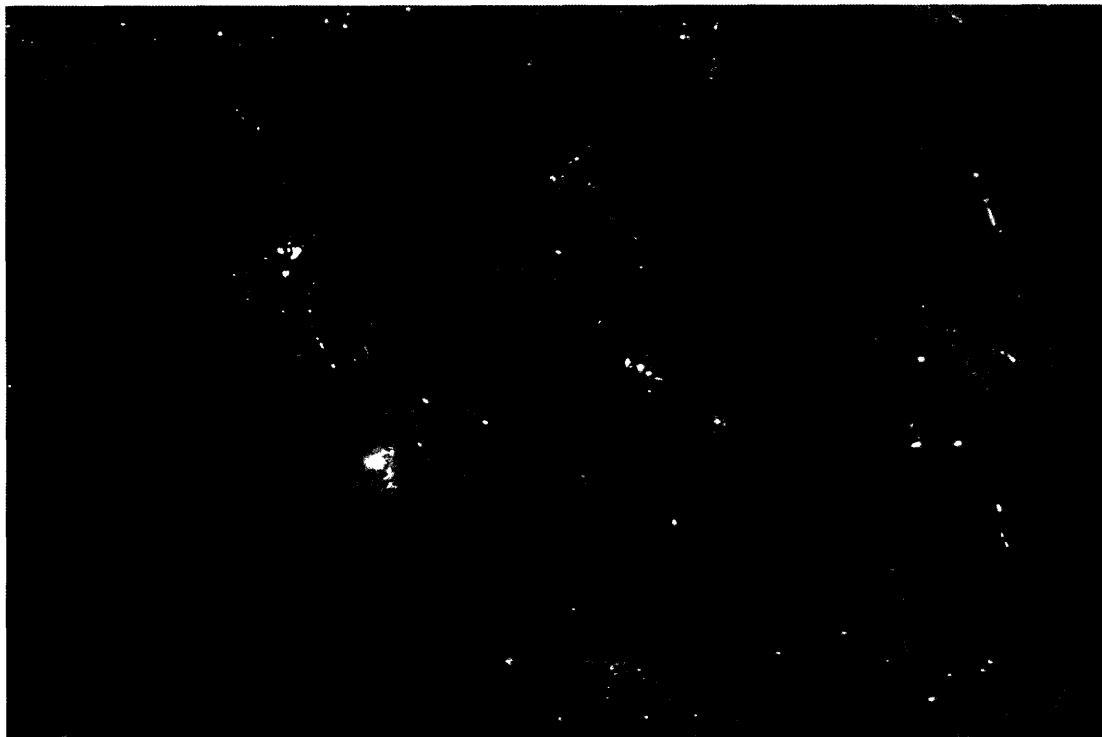
inhibited by increasing the thickness of the array, providing a greater surface area for viscous loss. The design can increase wall thickness between holes in the array, but this would lead to stagnation much faster than increasing the thickness of the array. The flow is also controlled by cross-sectional size of the square holes. The coolant should flow completely through the array, but slower than pure hydrostatic pressure would dictate.

The square holes were sized to 1 by 1 mm. At this size the flow rate was restricted, but allowed water to pass through freely and completely. There was no particular target flow rate, since the input flow rate has yet to be determined. The coolant input flow rate will still determine the flow rate across the capillaries. The laser engraver succeeded in forming a clean wall thickness of 500  $\mu\text{m}$ . Thinner walls began to melt due to the heat of the laser or were too brittle. Figure 5 shows the quality of machining of varying wall thickness under a microscope.

The laser engraver created clean square cuts in acrylic up to a thickness of 6 mm. Thicker stock created distorted arrays that either blocked the flow or did not provide sufficient surface area for restriction. Figure 6 shows the quality of the machining using varying stock thickness under a microscope.

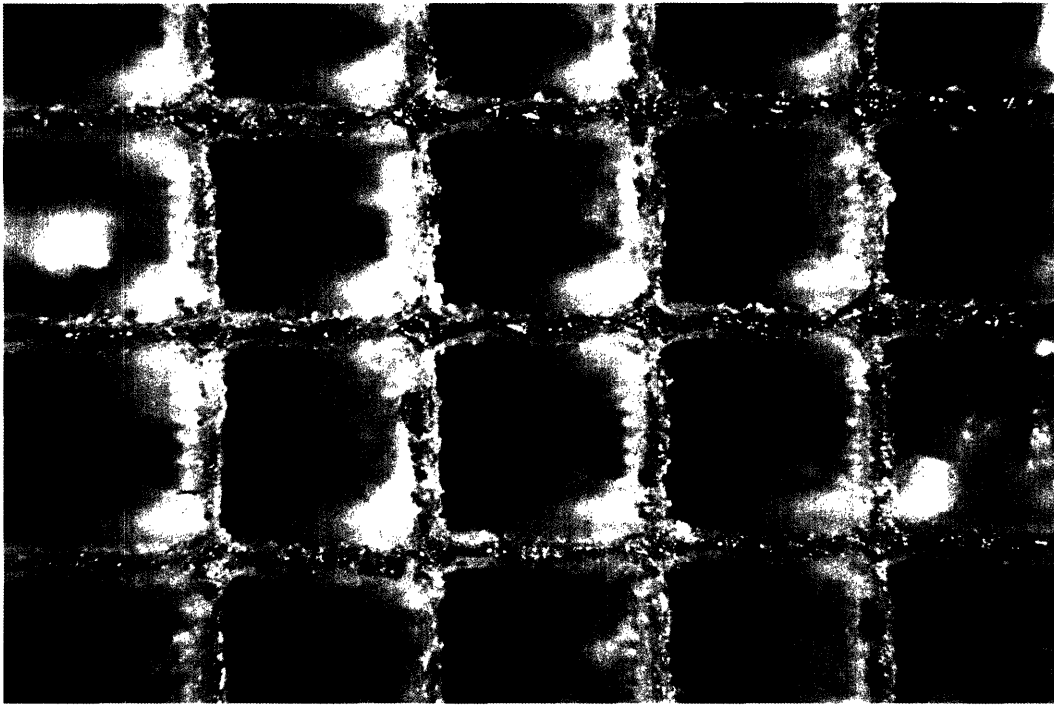


a)



b)

Figure 5: Flow restrictor arrays, 1 by 1 mm square holes a) 500  $\mu\text{m}$  wall thickness b) 250  $\mu\text{m}$  wall thickness.



a)



b)

Figure 6: Flow restrictor arrays, 1 by 1 mm square holes, 500  $\mu\text{m}$  wall thickness a) 6 mm stock b) 10 mm stock.

The final design for these flow restrictor arrays uses the limits of the laser machining as the specifications as shown in Figure 6a). The array is 50 mm high, the entire height of the module, and the square holes cover a length of 100 mm, as large as the width of the capillary array. The design, including a small border for mounting the slides, is shown in Figure 7.

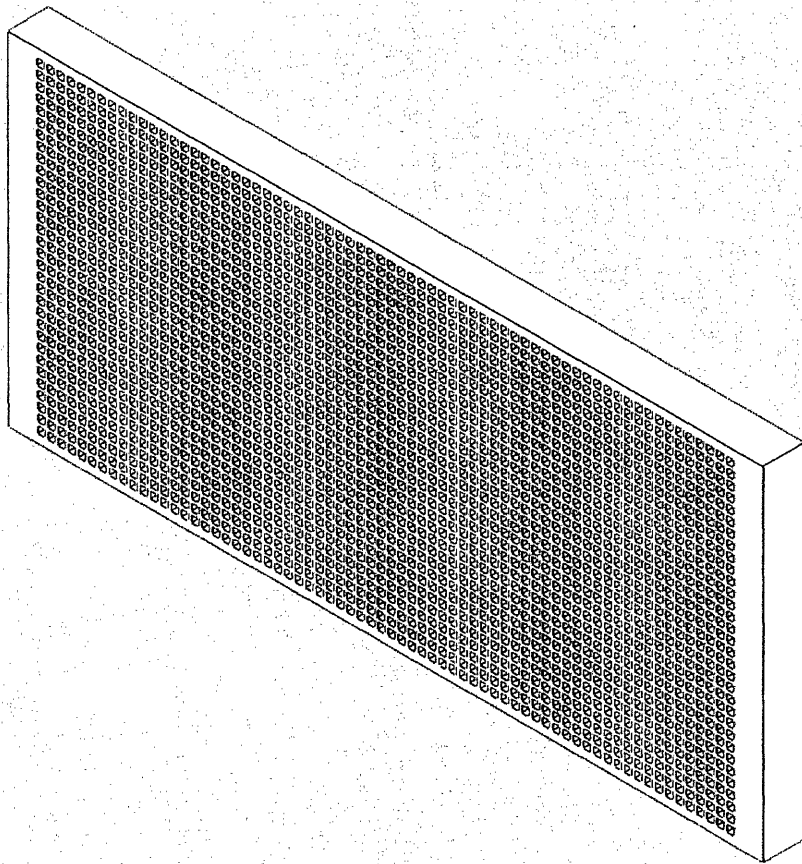


Figure 7: Flow restrictor array design.

The long, narrow passages create viscous resistance as the fluid passes through the restrictor array. The entrance flow rate from the recirculating bath will be greater than the exit flow rate of the array as long as the fluid can build up behind the array. Thus, the entire fluid entrance chamber will fill before the fluid passes completely

through the arrays. However, once the chamber is full, the fluid pressure will increase and force the coolant to flow faster through the arrays, until the flow reaches steady-state. Thus, the overall flow rate at steady-state is not restricted, but the flow will be approximately uniform between successive modules within the structure.

### **4.3 Main Module**

The main module was designed to hold both the capillary array and flow restrictor slides. The structure allows the flow of coolant across the length. The structure was designed to mount into a housing which is 250 by 250 mm in size at the base. The housing for the system was a set of four posts, 40 mm square, with the outer corners of the posts forming the 250 square base footprint. At this size, the housing is large enough to mount the LED array and camera detection equipment necessary to illuminate and view the ends of the capillaries at maximum density.

#### **4.3.1 Proof of Concept**

A preliminary design was constructed on the Viper stereo lithography apparatus (SLA) [1]. The capillary array was designed to mount flat in the bottom of the module. The flow restrictor arrays mount opposite each other in a vertical orientation in each of the two grooves. Coolant enters from one of the far indentations, flows across the capillary region, and exits through the other. A groove was created for a rubber o-ring, in order to seal the module to the one above it. The preliminary design and proof of concept are shown in Figure 8.

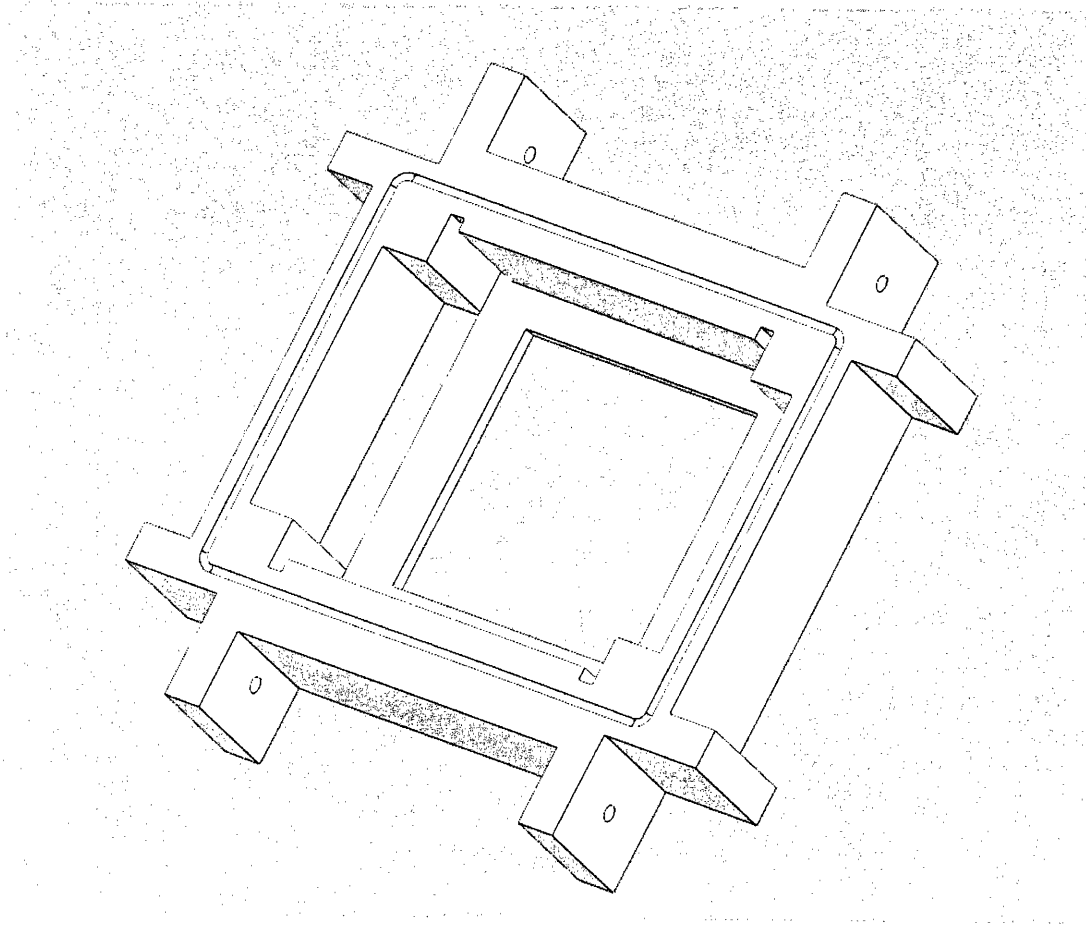


Figure 8a): Preliminary design of main module.

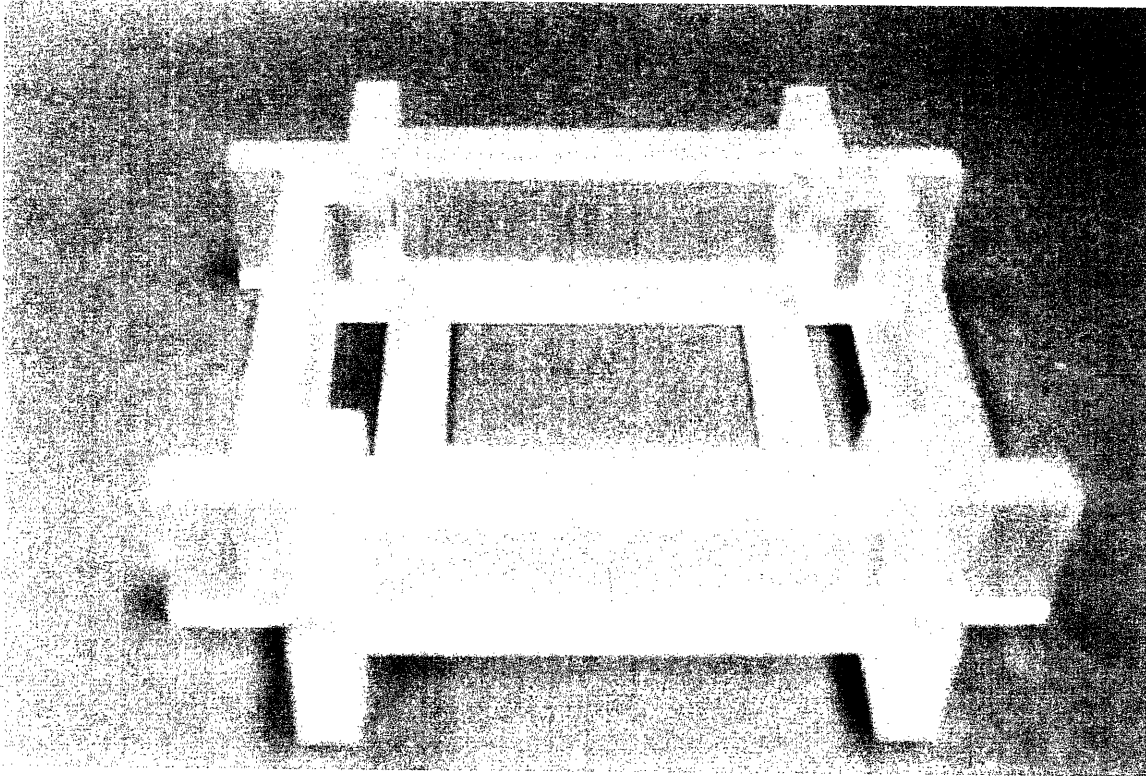


Figure 8b): Proof of concept of main module.

The SLA creates parts by laser-hardening a resin in differential layers. This manufacturing process is completely computer controlled, but is not a manufacturing choice for the module because of the low melting temperature of the resin. The resin begins to soften at 70 °C, and the instrument might require the coolant to run as hot as 80 °C. It should be noted that the softening temperature for acrylic is 90 °C, so the slides will not begin to lose structural rigidity even if the device operates at maximum temperature.

#### **4.3.2 Main Module Design**

The design for the main module used most of the features from the proof of concept, including the grooves for the flow restrictor arrays, a 3 by 2 mm rectangular groove locating the rubber o-ring, and the entrance and exit indentations for the flow of coolant. However, the preliminary design would have been difficult to manufacture, so

several features were altered. The flow restrictor arrays were held in place using set screws that enter from the side of the module. The capillary array was mounted in the midplane of the height of the module, held in place similarly by set screws. The design is shown in Figure 9.

Included in this design was a feature to connect the modules together. There is a pattern of bolt through-holes and tap holes around the border between the o-ring groove and the outer edge. The through-holes alternate with the tap holes. The through-holes also include a countersink for the head of the bolt. The closing pressure applied by a tightened bolt radiates from the head of the bolt downward at a 45 degree angle [19]. The module is 50 mm high, and there is a countersink of approximately 10 mm. Therefore, each bolt applies an approximately constant pressure in a circle of diameter 80 mm at the bottom surface of the module. The zones of applied pressure overlap as the bolt spacing between heads is 63 mm. This aids in creating a water-tight seal between modules.



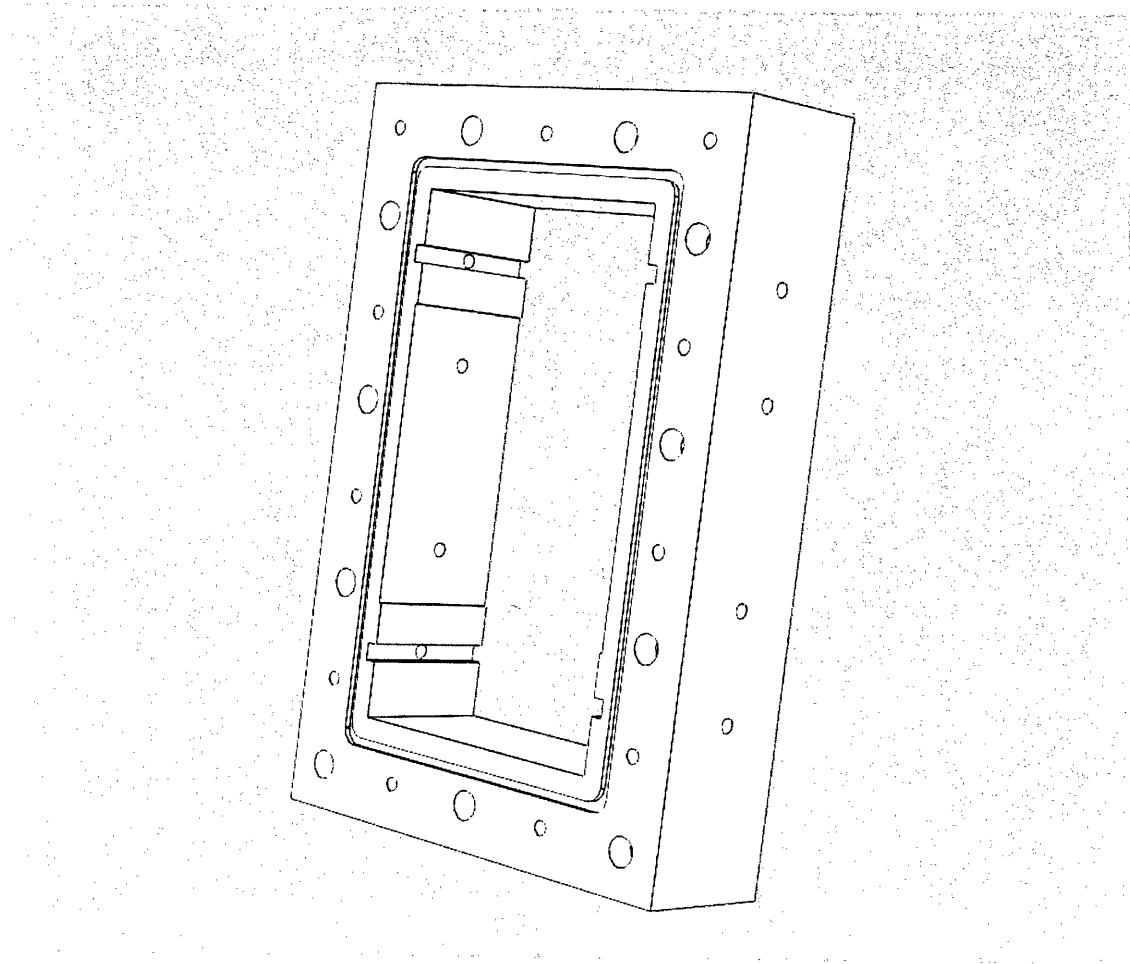


Figure 9: Main module design.

In designing for manufacture, each module has the same bolt-hole pattern. In order to bolt two together, one is rotated 180 degrees in the plane of the top surface. The through-holes of one align with the tap holes of the other. The pattern is illustrated in Figure 10.

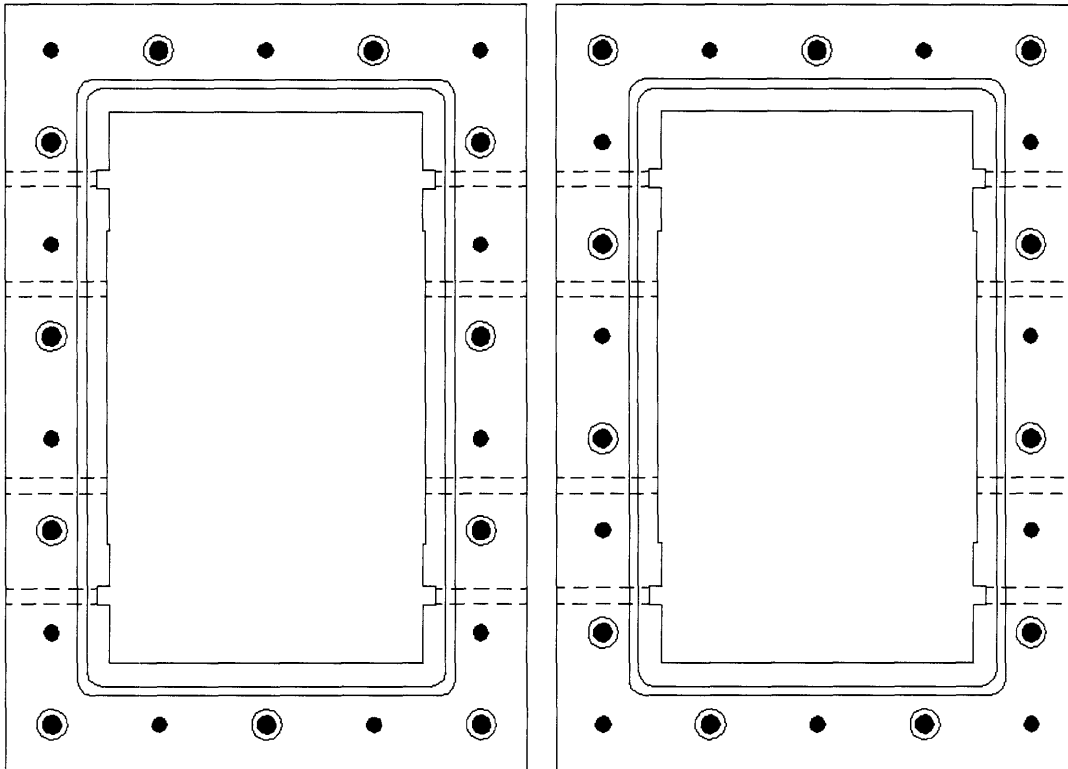


Figure 10: Bolt through-hole and tap hole pattern, the pattern is reversed to bolt two modules together.

Material considerations for this design were based on structural rigidity, machineability, and the thermal properties of the material. Plastics are difficult to machine and have poor thermal conductivity. The thermal conductivity of machineable ceramic is  $1.46 \times 10^{-3} \text{ kWm}^{-1}\text{K}^{-1}$  [9]. However, it is very difficult to machine without chipping or fragmenting. Also, machineable ceramic is very expensive; stock large enough to create a single module of this design would cost approximately \$4,000. Stainless steel has a thermal conductivity of  $12 \times 10^{-3} \text{ kWm}^{-1}\text{K}^{-1}$ , but is still costly and time-consuming to machine. Aluminum is relatively cheap, with stock large enough to machine costly roughly \$140, has a thermal conductivity of  $167 \times 10^{-3} \text{ kWm}^{-1}\text{K}^{-1}$ , and is significantly easier to machine than the other choices in terms of both operator skill and tooling.

The only concern with using aluminum as the material choice is the high coefficient of thermal expansion (CTE). If at maximum operating temperature the aluminum blocks will force the module to expand more than a few percent of the diameter of the rubber o-ring, leakage could occur. The CTE for aluminum is  $9.3 \mu\text{m}/\text{m}^{-1}\text{K}^{-1}$  [9]. The maximum operating temperature is approximately a 60 K change from ambient conditions and the height of each module is 50 mm. This results in a change in height of 0.028 mm total, which is less than 1% of the diameter of a 3 mm o-ring. Thermal expansion will not cause leakage problems.

Aluminum also has the tendency to corrode and oxidize, and the instrument is filled with flowing coolant. In order to prevent corrosion and protect the surface the design can be anodized after manufacture. Anodizing only adds approximately 10  $\mu\text{m}$  to the surface, so it will not interfere with the functionality of the design [19].

#### **4.4 Assembled Subunit**

The capillary array and flow restrictor arrays will mount into the main module as shown in Figure 11. Set screws tighten the arrays into the module and any number of subunits can be connected for a given length of electrophoretic excitation in intervals of 50 mm.

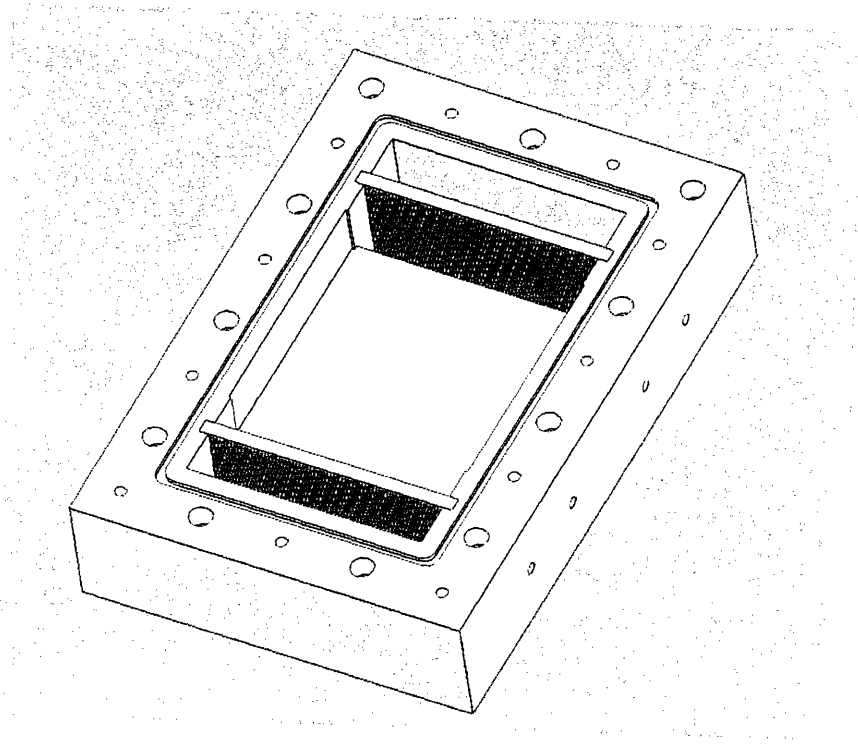


Figure 11: a) Assembled subunit with main module, capillary array, and flow restrictor arrays.

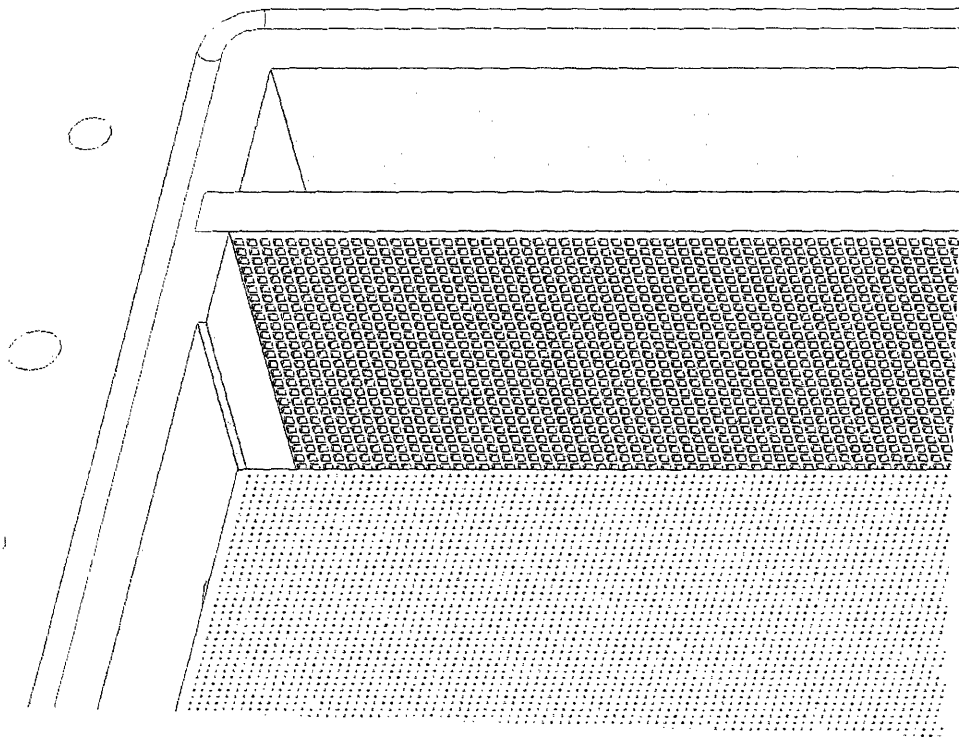


Figure 11: b) Close up of assembled subunit.

## 5.0 Manufacturing and Assembling the Subunit

The capillary arrays and the flow restrictor arrays were manufactured on the Trotec laser machining system, which offers better precision and accuracy than the Epilog system, and the main module was manufactured using a combination of computer numerically controlled (CNC) milling on the Haas VF-OE milling center and wire electric discharge machining (EDM) on the Charmilles Robofil 1020SI system [22,8,3]. The wire EDM pulses a high frequency current across a wire and uses the erosive effects of the discharge to machine [3]. All three manufacturing processes are controlled by computers; therefore a single operator can work on three separate parts at once. Each machine in the current configuration is capable of working only in a single plane without the operator reorienting the stock. The only machine that requires constant operator attention is the Microtap II tapping press, used for the holes in the main module [16]. The manufacturing stations are shown in Figures 12-15.

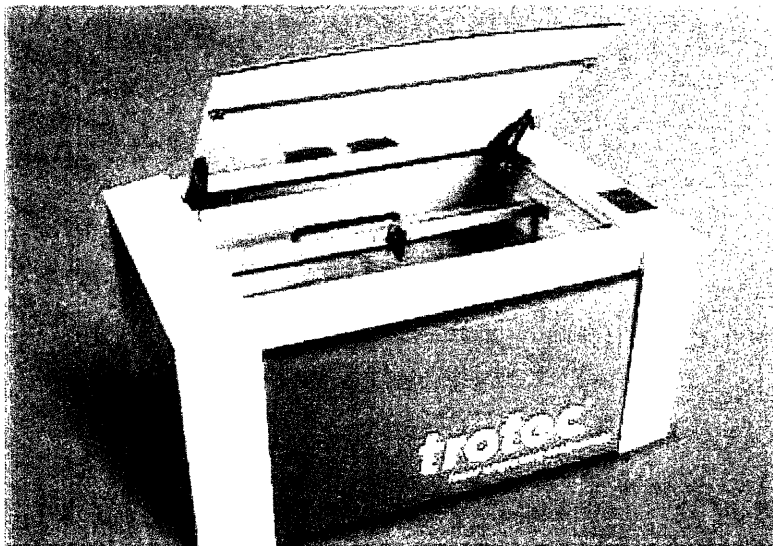


Figure 12: Trotec laser machining system [22].

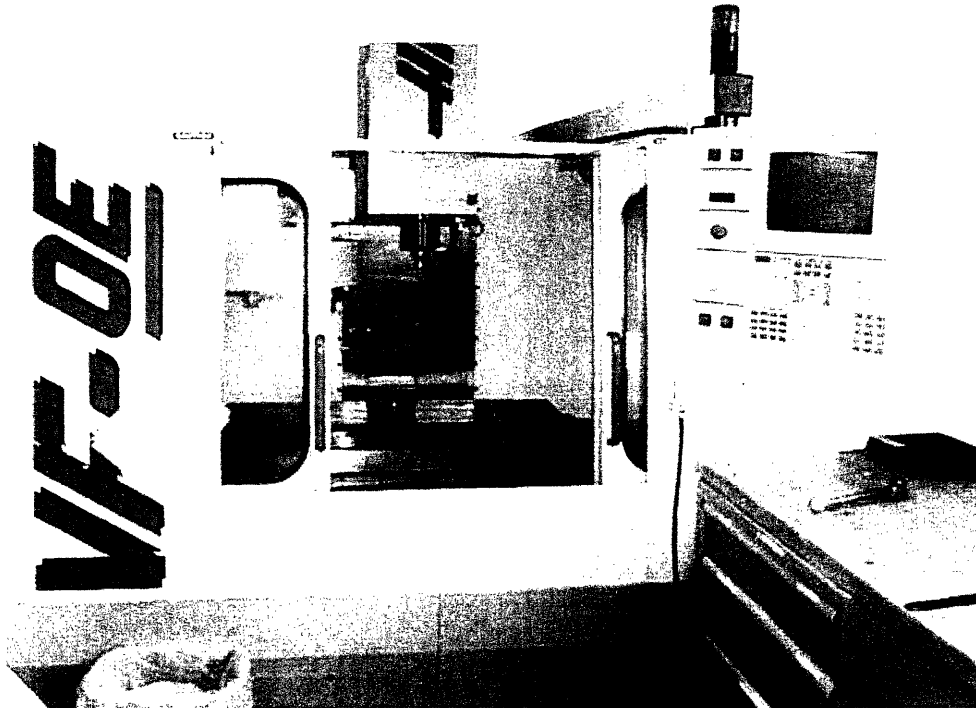


Figure 13: HASS milling center [8].

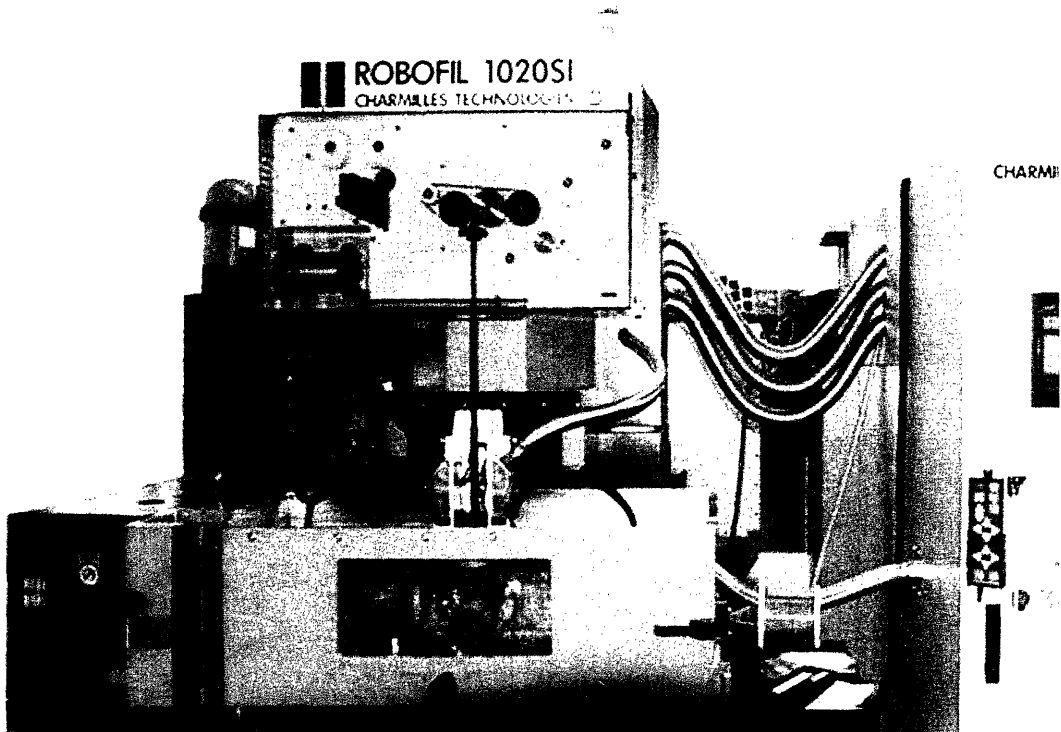


Figure 14: Charmlles wire EDM center [3].

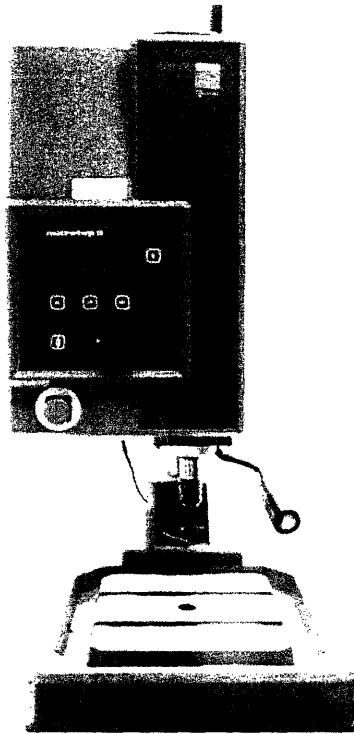


Figure 15: Microtap II tapping press [16].

### 5.1 Manufacturing the Capillary and Flow Restrictor Arrays

The designs for these slides were imported into the draft environment on the CAD software package. From the 2-D draft environment, the parts could simply be printed to the laser machining system using the computer communications port. The operator loaded the stock, and the laser engraver machines automatically without operator attention beyond general safety. The horizontal bed of the laser machining system can hold a piece of stock 700 mm by 400 mm so approximately 30 capillary arrays or 50 flow restrictor arrays can be machined at a time. Operator controls are primarily cutting speed, power, and beam frequency. Full power and heavily reduced speed at high cutting frequency produced the cleanest and fastest cuts. Each array, both capillary and flow restrictor, took approximately 25 minutes to machine. The machined parts are shown in Figure 16 and 17.

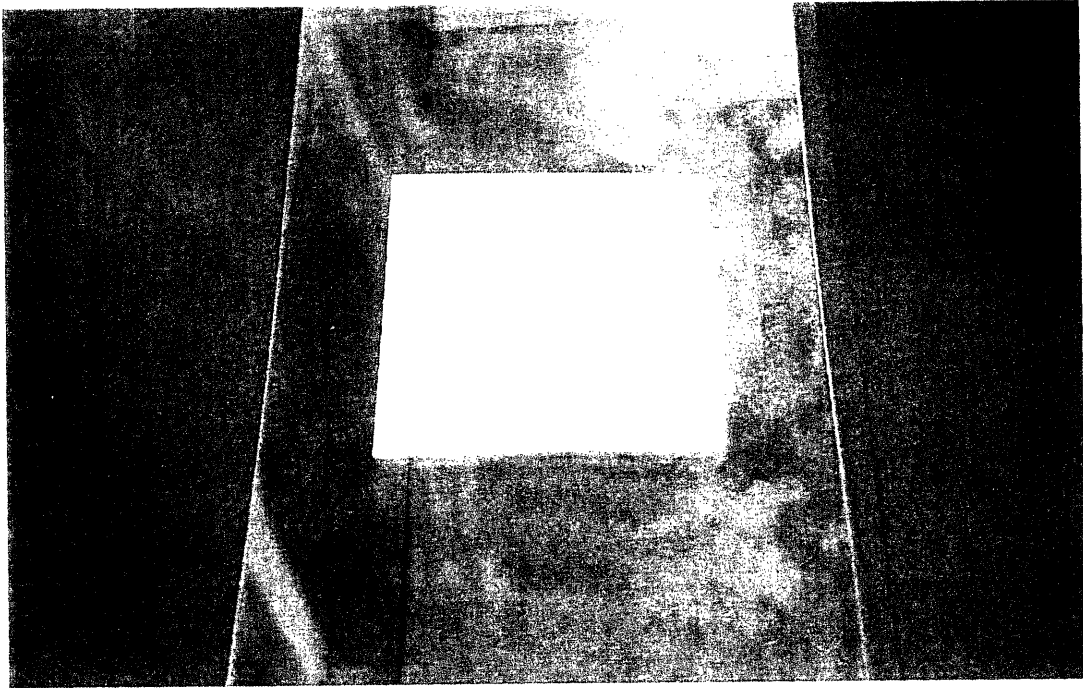


Figure 16: Machined capillary array.

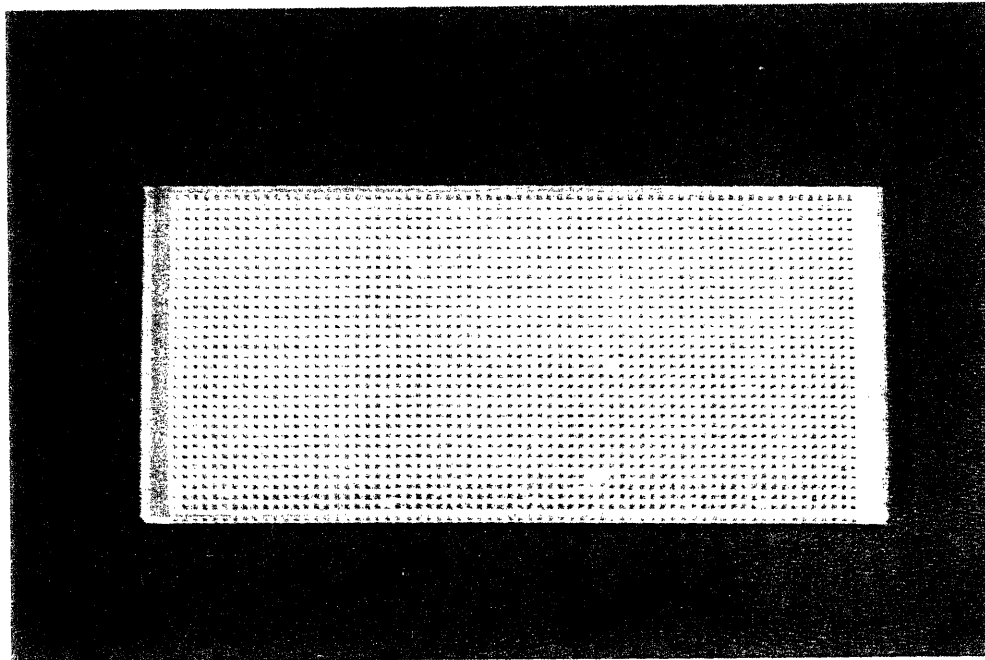


Figure 17: Machined flow restrictor array.



## **5.2 Manufacturing the Main Module**

The design for the main module was imported into the FeatureCAM computer-aided manufacturing software package, where the features were split into four distinct jobs [5]. The traces for the outer and inner borders of the design were machined on the wire EDM system and the holes and o-ring groove were machined using the milling center. For both machining centers, operator involvement included primarily fixturing the stock and locating an origin for the part in the machine. All cutting parameters are determined by the manufacturing software package.

The first job to manufacture the main module was to machine the outer border using the wire EDM. This took about 3 hours to machine, due to the thickness of the aluminum stock. Secondly, the rectangular block was fixtured into the milling center and the holes and o-ring groove were machined into the top face. This job necessarily was next in succession because the milling center also drills a pilot hole for the second wire EDM job. This job takes about an hour to machine, including the time to fixture the stock. Next, the inner border was machined on the wire EDM, taking approximately 3 hours as well. Following, the part was fixtured on either of its sides in order to machine the holes for the set screws that hold the arrays in place. This step requires more operator attention due to the speed of the job and the fact that it must be run twice for each part. The job takes approximately an hour. Finally, the tap holes in the top face and the side holes for the set screws must be tapped using the tap press. This took approximately an hour and was extremely labor-intensive.

Despite the fact that each part takes approximately 9 hours to manufacture, most of the jobs are not labor-intensive and a single operator can run 3 parts simultaneously,

one in each of the machining centers. Figure 18 shows a completed main module. The anodizing process was a contracted job. During anodizing, the aluminum modules were dyed blue.

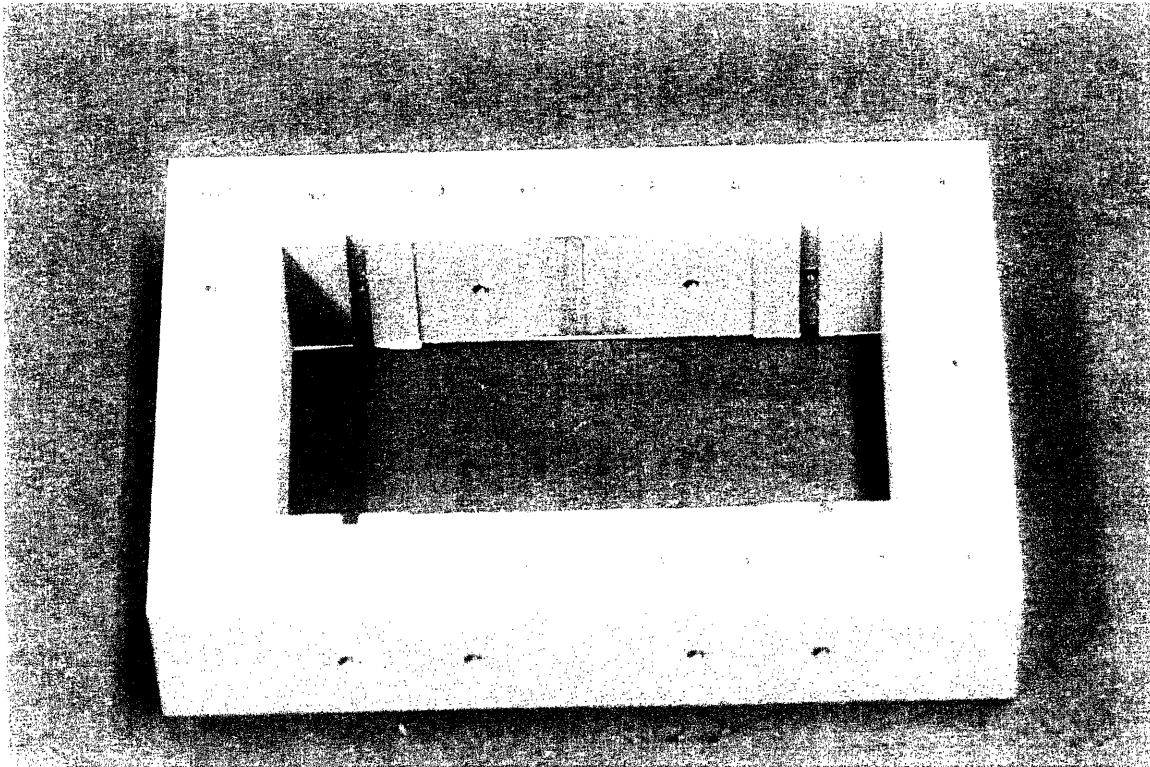


Figure 18: Machined main module before anodizing.

### **5.3 Assembling the Subunit**

Each subunit was assembled by hand, which included inserting the arrays into the module, cutting and greasing the o-rings, and bolting the assembled subunits together. An assembled subunit is shown in Figure 19. A prototype structure of length 300 mm, a complete six subunits, was constructed in total.

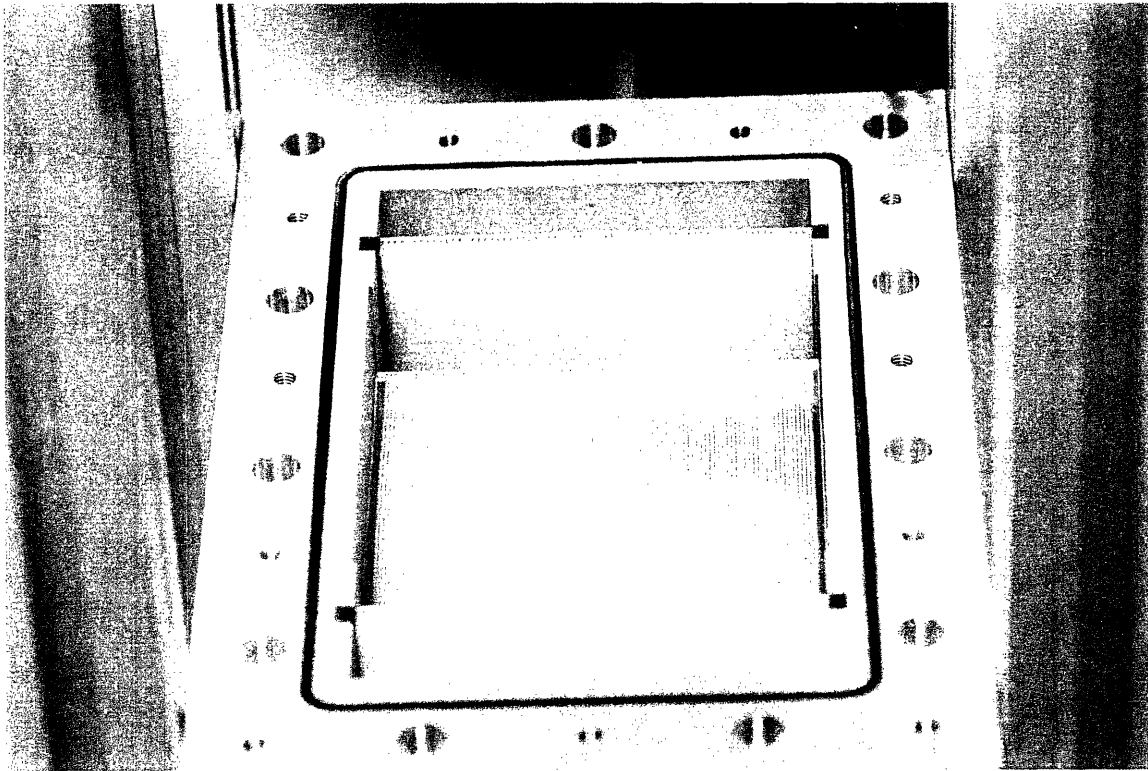


Figure 19: Assembled subunit with main module and arrays.

## 6.0 Testing of the Thermal Properties

Each capillary acts as an ohmic resistive heating element inside the main structure of the ultra high-throughput mutational spectrometer. It is currently uncertain how strict a level of temperature control is necessary in order to maintain constant denaturing within the capillaries. Regardless, thermal data must be collected to understand how the assembled structure behaves as the coolant flows through the modules. This simple test measures how much heat is lost by the device to the environment. The coolant enters the structure at a given input temperature and the coolant temperature is monitored through the structure and to the outlet.

### 6.1 Procedure

The thermal measurements were taken with a resistive thermal device (RTD). This device was chosen over the use of thermocouples because while thermocouples offer

structure is full of fluid. The experimental apparatus is shown in Figure 21 and Figure 22 shows a schematic of the placement of RTDs in the structure.

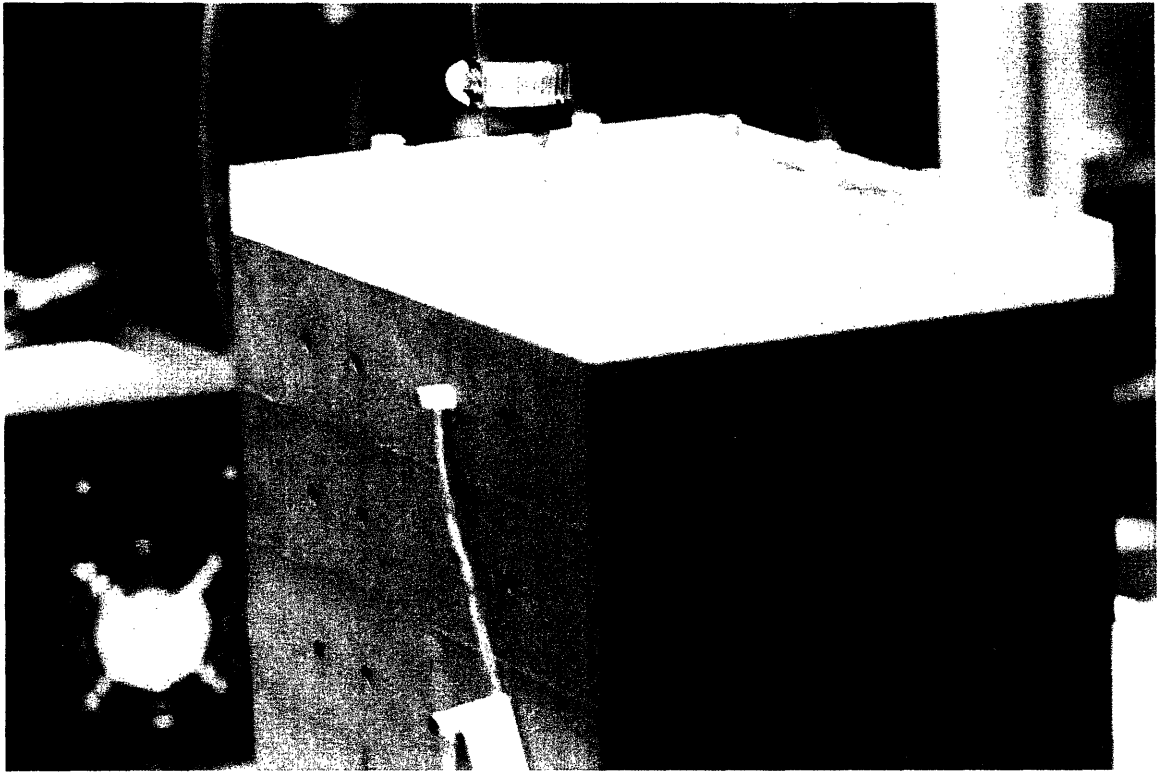


Figure 21: Experimental setup, including structure, endplates, and RTDs.

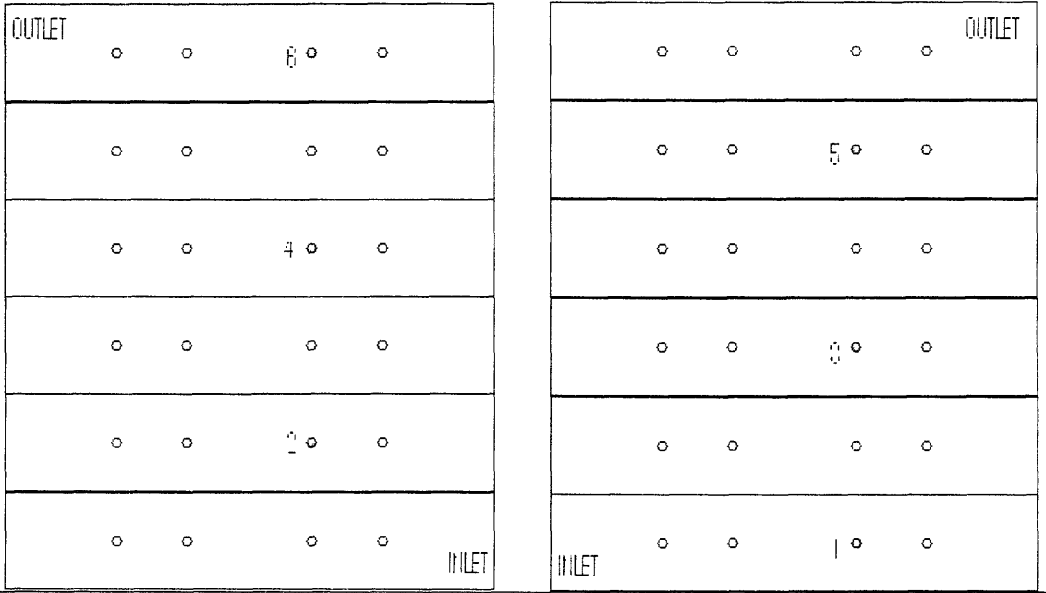


Figure 22: Schematic of RTD placement in experimental setup.

greater sensitivity and accuracy, they cannot be used over a large range of temperatures. The desired range of operating temperatures for this device is currently between 40 and 80 °C. Thermistors were a third choice, but too bulky for this application. The RTD offered the advantage of size, sufficient accuracy, and absolute calibration over the other thermal measurement choices. The RTD chosen was a 100 ohm device at 0 °C, approximately 2 mm square, with an operating temperature range of -50 to 600 °C and accuracy within 0.1 °C [18]. The RTD is shown in Figure 20.



Figure 20: Resistive thermal device (RTD).

The RTD was used in 4-wire configuration, where two of the wires make the necessary measurement and the other two leads sense the natural resistance of the wires and eliminate it from the signal. This measurement is more accurate than a simple two wire measurement. Seven RTDs were wired to a data collection unit, six were designated to the inside of the structure and the last measured the ambient temperature. The RTDs were mounted inside the structure through the holes for the set screws to hold the arrays in place. Using the symmetry of the design, one RTD was placed inside each subunit, on alternating corners.

Temporary endplates were fabricated for the structure, with the same bolt pattern as the main module and holes for pipe fittings to serve as the inlet and outlet for coolant. For the test, coolant will flow up from the bottom side and out the opposite side. This ensures that the recirculating coolant pump does not reach steady-state unless the entire

The coolant was allowed to flow from the recirculating water bath through the structure and reach steady-state. Both the large thermal mass of the structure and volume of fluid resist this temperature change. Once the temperatures equilibrated, the thermal measurements were recorded from the RTDs. For more complex experiments, the data acquisition can be computer controlled.

## **6.2 Results**

The first result of the thermal test was the success of the flow restrictor arrays. The coolant pump circulated with the top endplate missing and no outlet for the coolant. The entire inlet chamber filled completely and started to overflow before the coolant had significantly filled the capillary chamber. Thus, with the structure fully assembled, the flow across each of the modules was uniform despite hydrostatic pressure. Thus, with the structure completely filled and the top endplate in place, the flow rate was not restricted, but the flow was uniform across all six modules, despite greater hydrostatic pressure at the bottom of the structure.

The desired temperature for the thermal test was unable to be obtained with the available equipment. The thermal mass of the structure and the large volume of heat transfer fluid needed to fill both the structure and the recirculating water bath was too great to resist. Over the course of one hour, the recirculating water bath was only able to increase the outlet temperature of the fluid 1.0 °C. The bath temperature stagnated at this point, which was 24 °C. However, at this temperature, measurements for the RTDs were still recorded, as the temperature did reach steady-state. Also, the qualitative dynamic response was recorded as the temperature of the bath was increased.

The outlet temperature of the water bath dropped as it traveled through the transfer lines, but once the flow entered the structure, the variation was minimal. The variation between any two of the RTDs at any steady-state temperature was no more than 0.1 °C, the accuracy limit of the detection equipment. This apparent variation was constant between RTD 1, nearest the inlet of the flow, and RTD 5, nearest the outlet of the flow.

This variation can be reported as a percentage heat loss in terms of its temperature. Average temperature recorded from the series of RTDs was 23.4 °C. This results in a percentage temperature loss of 0.43 % across the length of the structure. The average path length of the flow was approximately 480 mm for six modules. Thus, the percentage temperature loss is 0.072 % on average for each module, which corresponds to an average path length of 230 mm.

As the recirculating water bath increased the temperature of the heat transfer fluid at a rate of approximately 0.1 °C every 5 minutes, the RTDs measured the dynamic response of the temperature profile inside the structure. The temperature change occurred first in RTDs 1 and 2, nearest the inlet to the flow and the bottom of the structure, and last in RTDs 5 and 6, nearest to the outlet and the top of the structure. The slower change occurred over the length of the structure, whereas the change in temperature over the height was aided by the effective impedance of the flow restrictor arrays. The time constant of the dynamic response was much faster than the rate of change of temperature of the heat transfer fluid. Thus, the difference in temperature between the series of RTDs was no more than 0.2 °C while the recirculating water bath increased the temperature of the coolant.

### 6.3 Discussion

The thermal tests were not performed inside the predicted operating temperature range for the device. The results are incomplete, but still partially characterize the thermal behavior of the structure. The temperature change inside the structure was minimal between the inlet and outlet, demonstrating little heat loss to the environment, despite the high thermal conductivity of aluminum. Thus, the thermal loss was in the large volume of heat transfer fluid necessary for the recirculating water bath and the transfer lines between the bath and the structure. Improvements in the design of the test would be to better insulate these transfer lines and possibly use another heat exchanger in conjunction with the bath, to reduce the strain on the equipment.

The percentage thermal loss for the six module structure can be scaled into the assumed operating temperature range for the instrument. The approximate loss is shown in Figure 23. This loss is only valid for the six module structure that has been constructed. However, the percentage thermal loss is directly proportional to the path length. Thus, the thermal loss can be related to the number of modules in the structure. This relation is shown in Figure 24.



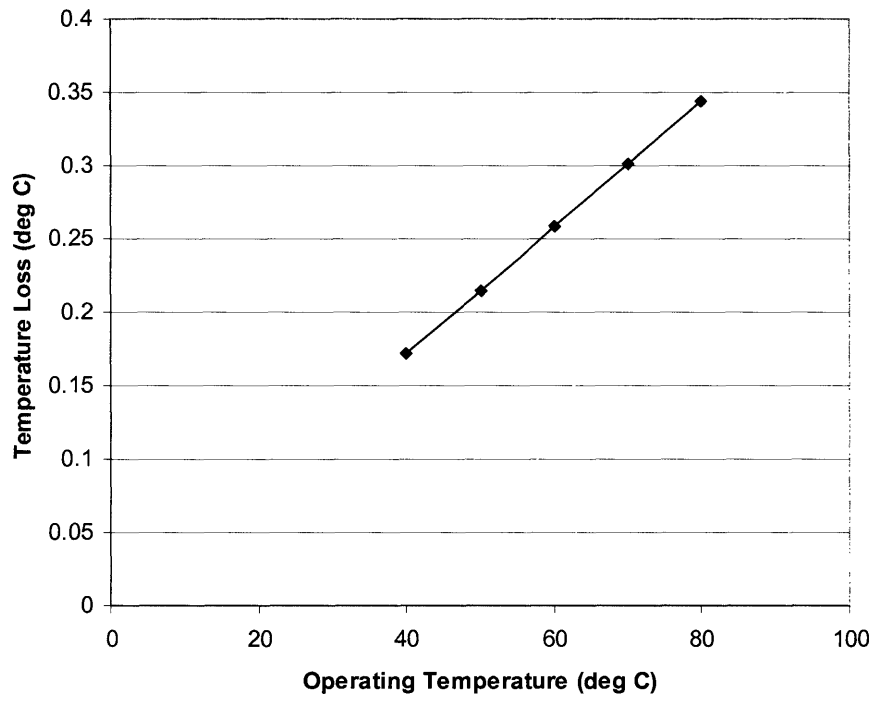


Figure 23: Temperature loss of six module structure running in assumed operating temperature range.

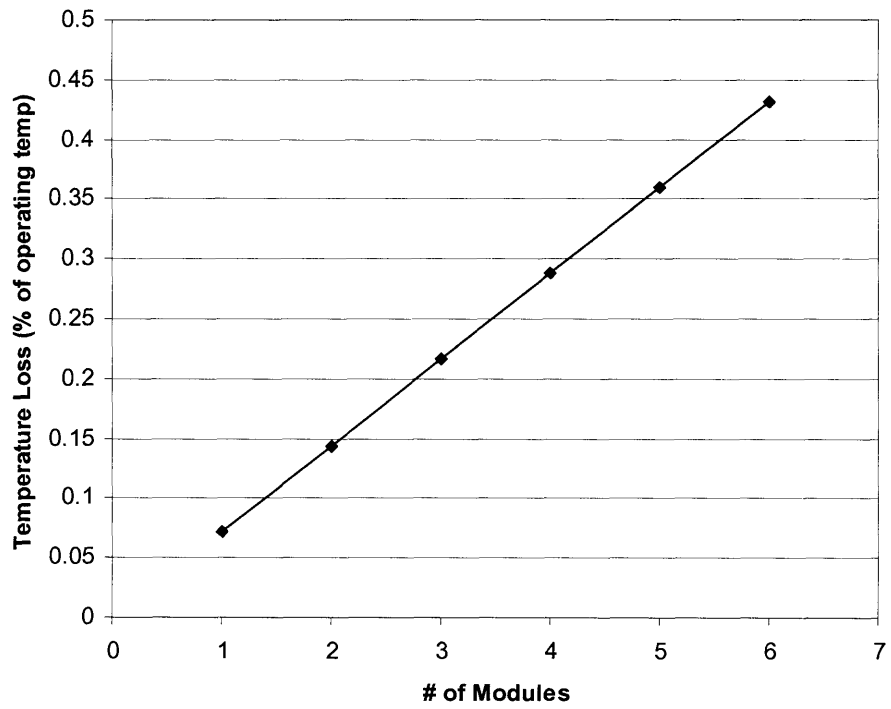


Figure 24: Temperature loss as a function of the number of modules in the structure.

## **7.0 Conclusion**

The design of the structure of ultra high throughput mutational spectrometer included both biological and manufacturing considerations. CDCE requires specific operating conditions, but in many cases the design was limited by geometry and the ability to machine effectively. The design for manufacturing was critical to the instrument, if the device is to reach the medical community.

## **7.1 Future Work**

The next steps for the structure involve more significant testing of the thermal properties. A series of heating elements must be added in order to measure the thermal response under more realistic operating conditions. The capillaries must be mounted into the arrays and a set of end-plates must be designed that allow the DNA samples to be loaded and detected. The basic structure is in place, must the assimilation of the structure into the instrument is the necessary next step.

## **Bibliography**

1. 3-D Systems, Valencia, California. <http://www.3dsystems.com>.
2. Apogee Instruments, Inc, Auburn, California. <http://www.ccd.com>.
3. Charmilles Technologies SA, Geneva, Switzerland. <http://www.charmilles.com>.
4. Crane, B., Hogan, C., Lerman, L. and Hunter, I.W. DNA mutation detection via fluorescence imaging in a spatial thermal gradient, capillary electrophoresis system. *Review of Scientific Instruments*. 2001 Nov; 72(11):4245-4251.
5. Engineering Geometry Systems, Salt Lake City, Utah. <http://www.enggeo.com>.
6. Epilog Laser, Golden, Colorado. <http://www.epiloglaser.com>.
7. Goetzinger, W., Kotler, L., Carrilho, E., Ruiz-Martinez, M.C., Salas-Solano, O. and Karger, B.L. Characterization of high molecular mass linear polyacrylamide powder prepared by emulsion polymerization as a replaceable polymer matrix for DNA sequencing by capillary electrophoresis. *Electrophoresis*. 1998; 19(2):242-248.
8. Haas Automation, Inc, Oxnard, California. <http://www.haascnc.com>.
9. Incropera, F. and DeWitt, D. *Fundamentals of Heat and Mass Transfer*: John Wiley and Sons; 2001.
10. Khrapko, K., Coller, H., Andre, P., Li, X.C., Foret, F., Belenky, A., Karger, B.L. and Thilly, W.G. Mutational Spectrometry without phenotypic selection: human mitochondrial DNA. *Nucleic Acis Research*. 1995;25(4):685-693.
11. Khrapko, K., Hanekamp, J.S., Thilly, W.G., Belenkii, A., Foret, F. and Karger, B.L. Constant denaturant capillary electrophoresis (CDCE): a high resolution approach to mutational analysis. *Nucleic Acids Research*. 1994; 22(3):364-369.
12. Lerman, L.S. and Frisch, H.L. Why does the electrophoretic mobility of DNA in gels vary with the length of the molecule? *Biopolymers*. 1982; 21(5):995-997.
13. Li, X.C., Khrapko, K., Andre, P.C., Marcelino, L.A., Karger, B.L. and Thilly, W.G. Applications of constant denaturant capillary electrophoresis/high-fidelity polymerase chain reaction to human genetic analysis. *Electrophoresis*. 1999; 20(6):1224-1232.
14. Li, X.C. and Thilly, W.G. Use of wide bore capillaries in constant denaturant capillary electrophoresis. *Electrophoresis*. 1996; 17(12):1884-1889.

15. Lim, E.L., Tomita, A.V., Thilly, W.G. and Polz, M.F. Combination of competitive quantitative PCR and constant-denaturant electrophoresis for high-resolution detection and enumeration of microbial cells. *AEM*. 2001; 67(9):3897-3903.
16. Microtap, Birmingham, UK. <http://www.microtap.com>.
17. Muniappan, B.P. and Thilly, W.G. Application of constant denaturant electrophoresis (CDCE) to mutation detection in humans. *Genetic Analysis* 1999; 14(5-6):221-227.
18. Omega Engineering, Stamford, Connecticut. <http://www.omega.com>.
19. Slocum, A. *Precision Machine Design*: Prentice Hall; 1992.
20. Stenesh, J. *Biochemistry*. New York: Plenum Publishing Corporation; 1998.
21. Thilly, W.G. Mutational spectrometry in animal toxicity testing. *Annual Review of Pharmacology and Toxicology*. 1990; 30:369-385.
22. Trotec Laser, Inc., Jackson, Missouri. <http://www.trotec.net>
23. UGS PLM Solutions, Plano, Texas. <http://www.solid-edge.com>.
24. White, F.M. *Fluid Mechanics*, Fourth Edition: WCB McGraw-Hill; 1999.
25. Xue, M.Z., Bonny, O., Morgenthaler, S., Bochud, M., Mooser, V., Thilly, W.G., Schild, L. and Leong-Morgenthaler, P.M. Use of constant denaturant capillary electrophoresis of pooled blood samples to identify single-nucleotide polymorphisms in the genes (Scnn 1a and Scnn 1b) encoding the alpha and beta subunits of the epithelial sodium channel. *Clinical Chemistry*. 2002; 48(5):718-728.